

PAPER • OPEN ACCESS

A measuring system for monitoring multi-nozzle spraying tools



To cite this article: Florian Schulz *et al* 2021 *Meas. Sci. Technol.* **32** 055902

View the [article online](#) for updates and enhancements.

You may also like

- [Spinodal de-wetting of light liquids on graphene](#)
Juan M Vanegas, David Peterson, Taras I Lakoba et al.
- [Empirical modelling of wetting patterns in a controlled drip irrigation system for sandy loam soils](#)
FA Rizqi, Murtiningrum and Ngadisih
- [Mortality among military participants at the 1957 PLUMBBOB nuclear weapons test series and from leukemia among participants at the SMOKY test](#)
Glyn G Caldwell, Matthew M Zack, Michael T Mumma et al.

A measuring system for monitoring multi-nozzle spraying tools

Florian Schulz¹ , Franziska Reincke¹, Matthias Mrochen² and Frank Beyrau¹ 

¹ Lehrstuhl für Technische Thermodynamik, Otto-von-Guericke-Universität Magdeburg, Magdeburg, Germany

² Fimro GmbH, Langenstein, Germany

E-mail: florian.schulz@ovgu.de

Received 27 August 2020, revised 19 January 2021

Accepted for publication 27 January 2021

Published 12 March 2021



CrossMark

Abstract

Spray tools with multi-nozzle-arrays are used in a wide variety of applications. Monitoring the functionality of complex spraying tools with a large number of individual nozzles is a great challenge. For this purpose, we have developed a measurement technique based on the wetting pattern, which forms on a surface during spray impingement. To investigate the performance of this measurement technique we applied a spraying tool with nine external mixing air-water nozzles, the geometric alignment of which can be freely adjusted. In the first test series, the precision of the evaluation of the nozzle alignment is determined. The second test series focuses on the individual sizes of the wetted areas. Here the reproducibility, the influences of the operating modes and the nozzle type were evaluated. Subsequently, the functionality is tested in an exemplary test case in which two of nine nozzles were readjusted in a defined manner. Finally, the wetting pattern resulting from injecting a full spray is discussed and the necessary image processing steps are provided. In summary, this measuring system allows efficient, fast and cost-effective control and documentation of the alignment and functionality of spraying tools, thereby avoiding production downtime and related costs.

Keywords: spray characterization, spraying tool monitoring, wetting pattern, frosted pane

(Some figures may appear in colour only in the online journal)

1. Introduction

In industrial processes, there are a variety of applications for spraying tools that are equipped with a large number of nozzles. A small sample with only nine nozzles is shown in figure 1. In foundry technology, such multi-nozzle spraying tools are used for cooling, cleaning or wetting of casting molds with a release agent. It is necessary that a spraying tool is adapted exactly to the geometry of a casting mold. To achieve the necessary flexibility in spraying tool design, the geometric alignment of the individual nozzles is usually freely adjustable. To fulfill its task perfectly, all nozzles

must be functional and correctly aligned (Miller and Butler Ellis 2000).

Under the harsh conditions prevailing in the casting industry, individual nozzles of a spraying tool can become dirty, clogged or change their geometric alignment. This will lead to inhomogeneous cooling, incomplete cleaning or incomplete wetting of the release agent. As a result, reject products are produced (Dannigkeit *et al* 2012) and production downtimes occur due to the maintenance work then required. In such a case, a technician checks and adjusts the spraying tool visually, which is very time-consuming, error-prone and often needs more than one iteration.

One possibility to avoid the high costs of failing spraying tools is to regularly maintain and readjust the nozzles, but this demands an applicable method to document the spray properties. In this case, it is not necessary to measure quantitative values like droplet sizes or mass fluxes. Rather, it must be determined whether spray properties such as the geometric



Original content from this work may be used under the terms of the [Creative Commons Attribution 4.0 licence](https://creativecommons.org/licenses/by/4.0/). Any further distribution of this work must maintain attribution to the author(s) and the title of the work, journal citation and DOI.



Figure 1. Multi-nozzle spraying tool.

alignment or the mass flow have changed. This can be done, for example, by comparing a current control recording with an original master recording.

At present, a multitude of measurement methods exist for the determination of specific spray properties, such as droplet velocity and diameter, spray beam width and penetration depth, spray density distribution or local mass flux distribution.

Phase Doppler anemometry (PDA) measurements are generally used to record droplet sizes and droplet velocities at a defined measuring position (Yokoi and Aizu 2009, Heldmann *et al* 2013). However, by systematically scanning a plane it is also possible to determine the spatial distribution of the spray. A prerequisite for the method is the optical accessibility of the measuring volume (von Deschwanen 2017, Rahim and Dorairaju 2018). If the path of the laser beams or the path of the resulting measurement signal is strongly influenced by interfering droplets, a measurement is not possible. For this reason, and because it would take a very long time to scan an entire nozzle field, it is not practical to use the PDA technique for the described measurement task.

The recording of shadow images or Mie-scattering images of the propagation of a spray is one of the standard methods to determine, for example, the width or the penetration of a spray (Kim *et al* 2018, Ainsalo *et al* 2019). This is very effective for individual spray jets or single nozzles. With nozzle-arrays with a large number of nozzles that are partly behind each other, it is difficult to evaluate results with this technique (Zelenak *et al* 2015, Lujaji *et al* 2016).

By using laser light sheets, regions within a spray, which are not accessible by means of shadowgraphs, can also be made optically accessible (Baetz *et al* 2005, Zhang *et al* 2012). A perpendicular cut through the spray jets can be used to determine spray positioning and in some cases to investigate the relative spray density. Since the laser-light is attenuated more and more as it travels through the spray this technique reaches its limits with large nozzle-arrays (Serras-Pereira *et al* 2015, Liu *et al* 2019a). Disadvantages of this technique are the high costs for the laser and the high sensitivity of the laser technology and optics to dirty environments. However, similar

to the PDA technology, the increased safety requirements for the use of lasers always have to be observed when operating such systems, which makes the practical use in foundries very difficult.

Another classical device for the characterization of sprays is a spray patternator, which can be used to determine the local mass flux (Dullenkopf *et al* 1998). For large nozzle arrays, equally large patternator surfaces with a large number of collection openings and with an automated readout of the collected water masses would be necessary. The challenges of such a system are the required high local resolution and the possibility of cleaning the patternator (Aísa *et al* 2002).

There is an earlier method that comes very close to the one presented here, the patterning of sprays with slides (Lefebvre and McDonell 2017). For the application, a solid surface—often glass—is covered with a rather loose coating. Here soot coatings from burned kerosene or magnesium were used (May 1950, Elkotb *et al* 1978). Thus, the impact of liquid on the surface leaves footprints. These traces can be so fine that it is even possible to determine the size of individual droplet impacts with the help of a microscope and thus draw conclusions about the droplet sizes. Disadvantages for the use for the described application are the difficult application with continuous sprays, the time-consuming preparation of individually coated surfaces and the lack of temporal resolution.

So far, no measuring method is specialized in the simultaneous acquisition of the geometric orientation of a large number of spray jets. In this paper a method for the characterization of the spray of nozzle-arrays is presented. It is based on the idea of the so-called refractive-index-matching (RIM) method. The RIM method uses the light scattering of the roughness of a surface to visualize the deposition of a transparent liquid on the surface (Shedd and Newell 1998, Fansler and Parrish 2015, Henkel *et al* 2016, Liu *et al* 2019b). For the setup, a frosted pane is positioned in front of the spraying tool. Then a short, simultaneous injection of all nozzles of the spray tool takes place. The spray jets impinge on the glass pane and wet it. Simultaneously, a camera detects the resulting pattern. This allows a comparison to be made between the current control recording and an original master recording made during commissioning (e.g. the beginning of the spray tool's life cycle) when the spray tool was functioning correctly. Deviations between the recordings indicate changes in the spraying tool and allow problems to be eliminated quickly. This measurement technique enables cost-effective and time-efficient testing of the alignment and functionality of the individual nozzles of spraying tools in order to avoid production downtime.

2. Material and methods

2.1. Setup and spraying tool

The basic configuration of the measuring system is shown in figure 2. The main component of the measuring system is a frosted glass pane in front of the spraying tool. The nozzles face the roughened side of the pane. For the fundamental research, a 3×3 nozzle-array was chosen to represent the general behavior of a spraying tool as it is used in the casting

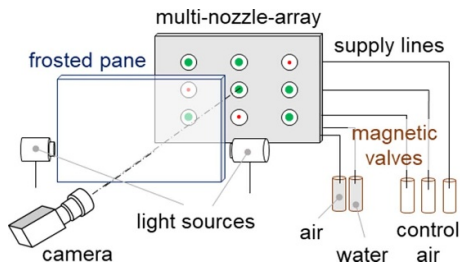


Figure 2. Scheme of the experimental setup, large nozzles in green and small nozzles in red.

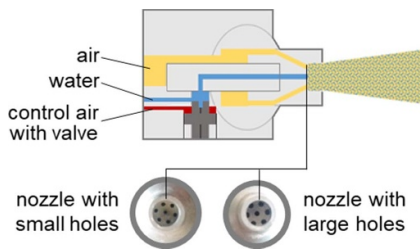


Figure 3. Operating principle of the external mixing air-water nozzles and photographs of two nozzles with different hole diameters; small and large nozzles with a diameter of 0.6 mm and 1 mm, respectively.

industry. The applied type of nozzle is an external mixing air-water nozzle (SD1 nozzles with part numbers 135.970 and 135.913 from Wollin GmbH), in which the atomization takes place by blowing in compressed air. The spraying tool has connections for air and water as well as the electrical wiring for the magnetic valves, which control the air and water inlet. To control the magnetic valves and thus open the air and water supply a triggering device, sending 5 V-TTL signals, is used.

Before an injection process, the air pressure and water pressure are only present up to the magnetic valves. By opening the valves, the pressure in the system rises rapidly. With the applied spraying tool, it is not possible to control each nozzle independently but it is possible to address the three rows (each with three nozzles) separately. By opening the magnetic valve for the control air of a row, the nozzle internal valves will open. These nozzle internal valves are responsible for opening the water flow. Due to the pneumatic characteristic of the internal valve, critical air pressure must first be reached before the valve opens. Figure 3 displays the operating principle of the nozzles.

Depending on the application, different kinds of nozzles can be installed simultaneously in real spraying tools. To simulate this, six nozzles with a large hole cross-section and three with a small hole cross-section are used. In figure 2, the nozzle arrangement is illustrated by the size and color of the points in the circles and photographs are shown in figure 3. To end the injection process, the magnetic valve for the control air is closed and the air pressure in the system is reduced via a drain valve until it falls below the critical pressure. Subsequently, the nozzle internal valves will close the water flow.

If the magnetic valve for the atomizing air supply stays closed, only a thin water jet will exit the nozzles. In this paper,

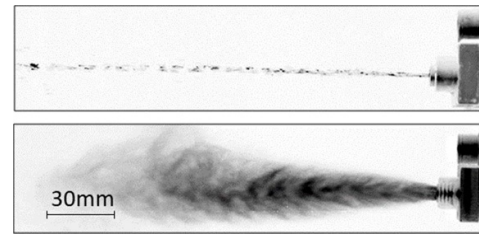


Figure 4. Mie-scattering image (negative image); top: injection of a straight water jet without the atomizing gas switched on and bottom: the resulting spray plume with atomizing air switched on.

such an injection is referred to as straight water injection. A spray will only be generated if the valve for the atomizing air supply is opened during the water injection. This is referred to as a spray injection. Example images of the generated spray as well as the straight water jet are given in figure 4. In the investigated example of the spraying tool for the casting industry, this property can be used for a deeper characterization of the spraying tool. For example, if only water jets are injected, the alignment of the nozzles and the functionality of the water-bearing system can be checked. If, in addition, a spray is generated, the measurement results also provide information about the functionality of the air-bearing system.

By using a compressor with an air reservoir, it is possible to preset the air pressure and to ensure that it remains constant. Similar to this, the water pressure is preset and kept constant with the help of an expansion vessel, while the gas side of the vessel is filled with nitrogen.

The basic settings are 5 bar for the air pressure and 4 bar for the water pressure while the air and water temperature are at equilibrium with the ambient temperature of 22 °C. The distance between the nozzle-array and the frosted pane is 11 cm. This distance is a compromise and was found in a preliminary investigation. From a metrological point of view, the smallest possible distance should be preferred. However, due to the geometric conditions of real nozzle arrays, these cannot be positioned arbitrarily to the glass pane.

In a standard sequence, the magnetic valve for the water supply opens first. Followed by the magnetic valves for the control air with an actuation duration of 150 ms. If the atomizing air is switched on, it is always applied simultaneously with the control air.

2.2. Measurement technique

During an injection process, the spray will impinge on the pane and produce an individual wetting pattern. This pattern is visualized by a camera, which is arranged frontally to the glass pane. To avoid negative effects of changing the camera alignment, the test setup was not changed during the experiments. A correction of changes in the camera orientation can be done via recording a calibration image (such as squared paper) and then to perform an image scaling and correction (Pan *et al* 2009). The camera used is a commercially low cost, Basler Ace acA1300-200um camera in combination with a wide-angle lens (Pentax-Rico C815B lens) with

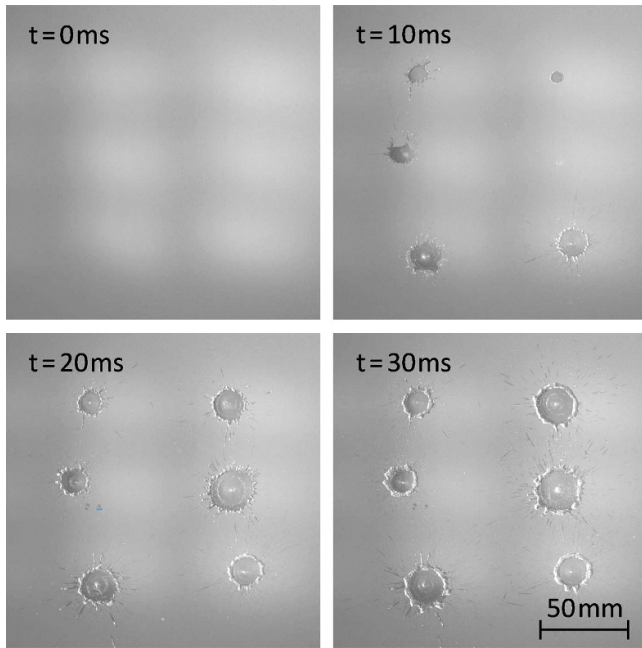


Figure 5. Series of raw images.

a fixed focal length of 8.5 mm. The resolution of the camera with 1280×1024 pixel results in a spatial image resolution of 0.2 mm/pixel. With the applied exposure time of 1 ms, no motion blur could be noticed. To achieve meaningful images with the necessary contrast, two LED Panels are used as light sources, while 50 Hz fluctuations were minimized using associated electronics. For later image evaluation, a homogeneous brightness distribution on the glass pane is of great importance. An example of an illuminated pane and an evolving wetting pattern is shown in figure 5.

2.3. Image processing

The method presented is based on the acquisition of wetting patterns. To be able to evaluate the positions and sizes of the individual wetted areas, it is necessary to prepare the recordings in a way that they can be evaluated. For this purpose, the algorithm used contains the following steps that are processed in sequence: reading the image data, filtering noise, normalization, binarization, closing holes, opening and determining the centers and sizes of the coherent wetted areas. Figure 6 shows an example of the illumination intensity distribution of an unwetted frosted pane (background), a raw image and the results of different processing steps.

2.3.1. Low-pass filter and normalization. Normalization is the fundamental step of the present image processing. Due to normalization, independence from illumination intensity and illumination inhomogeneity is achieved, such as uneven illumination or dirt on the pane. Therefore, normalization increases the robustness of the further evaluation against changing lighting (Serra 1982, Liu et al 2019c). For this processing step the intensity distribution of the illumination with the lights turned on is captured by recording the dry frosted pane before

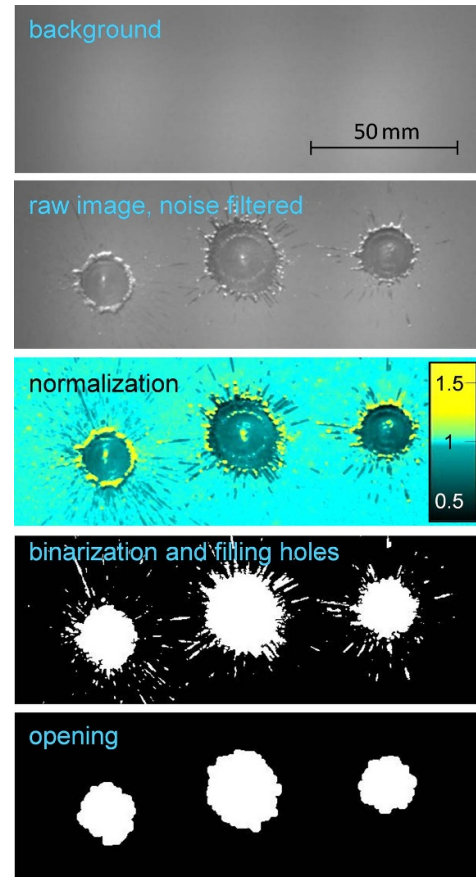


Figure 6. Visualization of the effects of image processing steps.

injection. In figure 6 this is referred to as background image. Subsequently, all images of the wetting process are divided by this background image. In regions without any spray impact, the resulting normalized image then should show an intensity value of one; in areas brighter than the initial image, values are greater than one and in darker areas, values are less than one.

Unfortunately, the images are afflicted with noise, which is originated in thermal noise and the read-out noise of the CMOS-Sensor, among others. Since the division (background/wetting image) in the normalization process is based on single pixels, the noise leads to the fact that even in areas where no wetting occurs values unequal to one will occur. This hinders the process of wetting pattern recognition. Therefore, a low pass filter is applied before normalization in order to reduce the existing noise. At the same time, the filtering should blur the boundaries of the wetting areas as little as possible. Therefore, the choice of the filter algorithm is dependent on noise and spatial resolution. With these requirements, a Gaussian filter with a rotationally symmetric kernel with a small diameter of three pixels and a standard deviation of 0.8 is applied. This relatively mild filtering—focusing on pixel-to-pixel noise and preserving the object edges—has proven to be sufficient for the present setup. Additionally, the use of a small kernel minimizes processing costs. In case of intense noise, the standard deviation of the Gaussian filter can be increased or more sophisticated denoising algorithms might be applied

(Beygi *et al* 2012, Mafi *et al* 2019). Regardless of this, the remaining noise is later removed by an erosion process.

During commissioning, care should be taken to ensure that the illumination on the frosted pane is as homogeneous as possible and that the intensity is in a range between 50% and 70% of sensor saturation. The relatively high illumination intensity increases the signal-to-noise ratio. At the same time, this range of intensity prevents that reflections—that occur on the surface during the injection process—are leading to oversaturation of the sensor.

2.3.2. Binarization. During binarization, the images are transformed into binary images with the help of a threshold value (Steinmüller 2008). Due to the former normalization, in the present case two threshold values are necessary: one threshold value above and one below one. Unfortunately, there are effects, which cause the unwetted regions to slightly change their brightness during the recording and wetting process. These are mainly reflections from the spray jets or shadows from the spray jets, which occur during the injection. Therefore, the threshold values must be selected with some distance to one. As a result, areas with values close to one are set to zero and areas where a significant intensity change occurs are set to one.

In general, the threshold values must be carefully selected when the measuring system is commissioned for the first time. Since two threshold values are required, the standard methods for determining an optimal threshold value, such as Otsu's method (Lazzaro and Ianniello 2018), cannot be used. Here, the threshold values of 0.9 and 1.2 are used for binarization. Due to the previously performed normalization, the threshold values represent a ratio of the change of light intensity of a 10% decrease and 20% increase, respectively. In our experience, this procedure is relatively robust against changes in the experimental setup or the illumination intensity. Likewise, these values should lead to good results in comparable experimental setups. In very unfavorable conditions it may be necessary to use more complex binarization methods, such as local thresholds (ImochaSingh *et al* 2012).

2.3.3. Filling holes. There are regions in the wetted areas which have values close to one. Thus, these areas are classified as dry due to the binarization and they appear as holes inside a wetted region. Therefore, the holes are closed by a flood-fill operation using Matlab 'imfill' function (Khudeev 2005). The result of binarization and filling holes is shown in the fourth picture in figure 6. For similar setups, the robustness against intensity irregularities can be increased by the closing of openings at the outer circumferences of the wetting regions. This operation must be performed before the filling operation and consists of a successive dilation and erosion with the same structural element (Paredes-Orta *et al* 2019).

2.3.4. Opening. The binarized image (figure 6) contains many small splashes. To extract the main impingement areas, the splashes can be removed with an opening function. For the opening operation, erosion and dilation are performed successively using the same structural element (Kumar and

Shunmugam 2006, Steinmüller 2008). With erosion, all detected wetted surfaces whose geometric dimensions are smaller than those of the eroding structural element are eliminated, this contains remaining noise. Therefore, the structural element must be at least as big as the diameter of the biggest splash, whereby 'diameter' refers to the smallest geometric expansion within the splash area. In the present experiments the splashes did not exceed 4.5 mm. Due to our spatial resolution of 0.2 mm/pixel a circular structural element with a radius of 12 pixels (2.4 mm) was applied in the present evaluation. Since the erosion leads to a reduction in the sizes of the main impingement areas, the previously subtracted pixels are added again by a dilation process afterward. The two operations are performed in Matlab using the 'imerode' and 'imdilate' commands.

2.3.5. Determination of the position of the centers and the size of the areas. The spray jets of the different nozzles of a nozzle-array do not hit the glass pane at the same time, as shown in figure 5. Therefore, within a series of images, it must be examined at which time step all jets impinged on the glass pane. The algorithm detects the existing wetted areas in each image of a series. The last image after which no further wetted area is added is used for the evaluation.

The size of the areas is simply determined by counting the number of pixels and multiplying them with the area they represent. The resolution of the recorded images might influence the determined area size. In the present case with a pixel area of 0.04 mm² and a size of the wetted area bigger than 200 mm², a single pixel adds less than 0.02% to the overall area.

The center of a wetted surface is determined as the centroid of the detected area, which means that the influence of an individual pixel on the overall position of the center is weighted with its distance from the center. The horizontal center (*x*-direction) and the vertical center (*y*-direction) are listed separately. Considering the accuracy, the maximum possible inaccuracy for e.g. a single horizontal line of pixels is half the width of a pixel. However, since the value for e.g. the horizontal center is not only determined from a single horizontal line but over the entire height of the wetted area, the accuracy here is much higher and the error tends towards zero due to an assumed normal distribution of the single line center deviations. Therefore, the resolution has no significant effect on the resulting center positions in the present application.

In the simplest case, the Matlab-function 'regionprops' with the selections 'centroid' and 'area' finds both properties from the processed images (Nazlibilek *et al* 2014). Since the wetted area becomes larger and larger with increasing injection time, the area calculation is carried out for the entire injection duration. Figure 7 shows an example of the evaluation of the centers of the examined image series, while the circle centers are identical with the centers of the wetted areas.

3. Results and discussion

In the series of experiments, two main properties of the wetting pattern are investigated, one being the centers of the wetted areas and the other being the size of the wetted areas. As

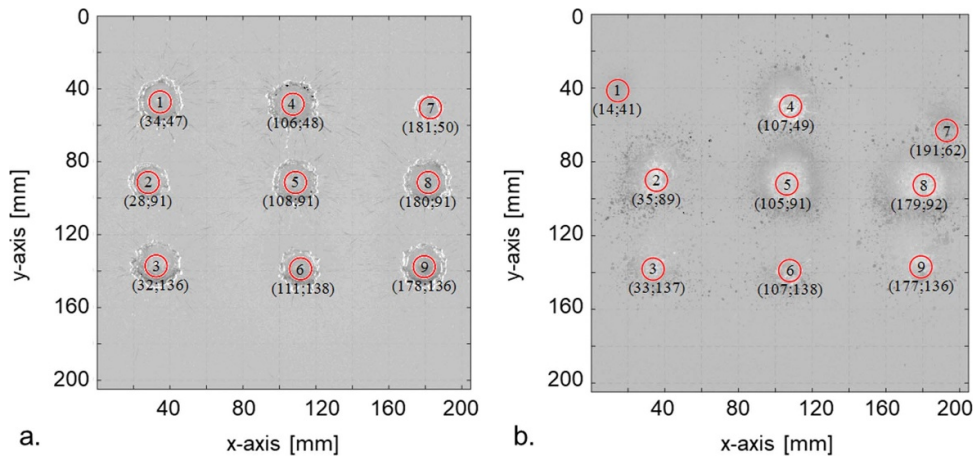


Figure 7. (a) Determination of the centers of the wetted areas for the injection of a straight water jet; (b) determination of the centers of the wetted areas of spray jets.

discussed in the previous section, the area centers and area sizes can be determined in a single image with very high accuracy. Now it is crucial to find out how much these values vary from injection to injection. Only, if the measurement results are reproducible, the new method can be used to detect malfunctions. The smaller the deviations from injection to injection are, the fewer repetitions are necessary to detect possible malfunctions. Therefore, we determine the associated standard deviations.

The area centers and area sizes can be evaluated for the injection of a straight water jet as well as for the injection of a full spray. The extracted parameters allow conclusions to be drawn about changes in nozzle orientation and flow rate. The results are discussed in the following. First of all, the precision of the center point determination of the individually wetted surfaces during the injection of a straight water jet as well as the injection of a spray are determined. Subsequently, the results of a controlled test case are presented. Here it is shown how precisely a geometric displacement of individual nozzles can be determined. In the third test-series of the investigation, the precision of the determination of the size of the wetted areas is analyzed.

3.1. Determination of the centers of the wetted areas

The centers of the wetting areas were always determined directly when all jets have reached the pane surface. This is about 40 ms after the beginning of the wetting of the frosted pane. The measurement is carried out for the injection of a straight water jet and as well for the spray injection including the atomizing air, while the air pressure is set to 5 bar and the water pressure to 4 bar. In the case of atomization, the atomizing air valve is opened at the same time as the control air valve. This timing is chosen because there is no effect on the impact of the spray jets when the atomizing air valve is previously opened. The recording of the injection process is repeated ten times for both cases, followed by the image processing and the determination of the center points.

The resulting positions of the center points are displayed in figure 7. The positions of the centers are shown using a

Cartesian coordinate system with the origin of the coordinates in the upper left-hand corner. The abscissa and the ordinate run from 0 to 203 mm. The wetting patterns in the background are the first images in which all jets have wetted the pane.

The mean values of the calculated positions of the center points for the straight water injection are given in table 1. Besides, the associated standard deviations resulting from repeating the tests ten times under constant conditions are given. The maximum deviation is 0.33 mm in x -direction and 0.35 mm in y -direction. The minimum deviations are 0.12 mm and 0.14 mm. There are no significant differences between large and small nozzles, nor are there any trends. Accordingly, the positions of the centers do hardly scatter from injection to injection when injecting pure water.

Considering a normal distribution of the measured values, a single measurement occurs with a high probability of 95.45% within a range of twice the standard deviation σ around the mean value. Transferring this to the present study, it can be assumed that there is a nozzle misalignment or problems in the water-bearing system, if the change in center-position for a single injection is larger than 0.7 mm (this corresponds to $2 \cdot \sigma_{\max}$). Based on our experience, this determination of the center point is very sensitive, many times more sensitive than the visual adjustment by a technician. If even smaller changes are relevant, repeated injections must be made and an average value must be calculated.

The results of the center determination for the spray injection with the associated standard deviations are shown in table 2. Again, this involves ten repetitions. It can be seen that the standard deviations are larger in comparison to the straight water injection. Especially the nozzle of the second column in the third row and the nozzles of the first column show larger standard deviations. The deviations from the centers vary between 0.37–2.18 mm in x -direction and 0.30–2.23 mm in y -direction.

Since no changes have been made to the system and all parameters have been kept constant, the positions of the center points of the spray injection can be compared directly with those of the straight water injection. Table 3 shows the differences between the average center positions in x - and

Table 1. Mean values of center points and standard deviations for straight water injection; in brackets: x - and y -positions in relation to the central wetted area (in second column and second row).

Column	Row	Nozzle holes	x -axis (mm)	σ_x (mm)	y -axis (mm)	σ_y (mm)
1	1	Large	34.3 (−73.5)	0.21	46.6 (−44)	0.31
	2	Small	27.9 (−79.9)	0.17	90.4 (−0.2)	0.25
	3	Large	32.5 (−75.3)	0.33	135.9 (+45.3)	0.35
2	1	Large	106.6 (+1.2)	0.22	47.7 (−42.9)	0.22
	2	Large	107.8 (0)	0.24	90.6 (0)	0.26
	3	Small	110.5 (+2.7)	0.31	137.6 (+47)	0.23
3	1	Small	180.7 (+72.9)	0.23	50.2 (−40.4)	0.22
	2	Large	180.2 (+72.4)	0.12	90.9 (+0.3)	0.20
	3	Large	178.1 (+70.3)	0.20	136.5 (+45.9)	0.14

Table 2. Mean values of center points and standard deviations for spray injection; in brackets: x - and y -positions in relation to the central wetting area (in second column and second row).

Column	Row	Nozzle holes	x -axis (mm)	σ_x (mm)	y -axis (mm)	σ_y (mm)
1	1	Large	18.7 (−87.8)	0.96	44.3 (−44.9)	2.09
	2	Small	34.2 (−72.3)	0.84	90.8 (+1.6)	1.38
	3	Large	30.5 (−76)	1.17	139.0 (+49.8)	2.23
2	1	Large	105.1 (−1.4)	1.00	48.0 (−41.2)	1.14
	2	Large	106.5 (0)	0.60	89.2 (0)	0.99
	3	Small	99.8 (−6.7)	1.39	140.5 (+51.3)	0.93
3	1	Small	186.4 (+79.9)	0.91	66.3 (−22.9)	1.12
	2	Large	174.8 (+68.3)	0.37	92.9 (+3.7)	1.29
	3	Large	179.3 (+72.8)	1.09	127.1 (+37.9)	1.56

Table 3. Comparison of the average positions of the center points for straight water and spray injection.

Column	Row	Nozzle hole	Δx (mm)	Δy (mm)
1	1	Large	−15.6	−2.3
	2	Small	+6.3	+0.4
	3	Large	−2.0	+3.1
2	1	Large	−1.5	+0.3
	2	Large	−1.3	−1.4
	3	Small	−10.7	+2.9
3	1	Small	+5.7	+2.0
	2	Large	−5.4	+2.0
	3	Large	+1.2	−9.4

y -direction. Here, the center points of water injection are assumed as the original position. The differences are particularly large in x -direction. The nozzle of the first column and first row and for the nozzle of the second column and third row has the largest distance with 15.6 mm and 10.7 mm.

The other distances are between ± 0.3 mm and ± 6.3 mm. Reasons for the deviations are the much larger wetting areas, due to atomization process. In particular, it is the air supply that causes a strong change in the direction of the water jet. Large deviations between spray and water jet lead to the assumption that the airflow through the air-bearing holes is not uniform and thus causes the spray to drift.

It can be summarized that the center points of the spray injection allow a statement about a nozzle alignment and the condition of the air bearing channels. Considering a single injection position changes from 4.5 mm ($2 \cdot \sigma_{\max}$ in table 2) are

significant. For the detection of smaller changes in center position, repeat tests must be carried out.

It can be concluded that combining the results of straight water injection and spray injection will allow additional analysis. If a similar change in the center position of a wetting area occurs with straight water injection and spray injection, it is too likely that this is due to a nozzle misalignment. On the other hand, if a relevant change in the center position of the wetting area only occurs in one operation mode, the fault is probably in the water-bearing system or the air-bearing system, respectively.

3.2. Controlled test case

To test the measuring method, the alignment of two nozzles was manipulated. The alignment of the nozzle of the second column and the first row was moved slightly to the lower left and the alignment of the nozzle of the third column and second row was moved to the upper left.

Metal pins were attached to the nozzles to document the adjustment of the nozzles. Then photos were taken from the side and from above, before and after the adjustment. Figure 8 shows an exemplary picture where the before and after pictures are superimposed. With these photos, the adjustment angles and thus the theoretically resulting changes of the centers of the wetted areas can be determined. The measured adjustment angles, as well as the resulting theoretical changes in position of the centers in x - and y -direction, are documented for both nozzles in table 4.

Table 4. Changes in the position of the center points for the two adjusted nozzles; left: theoretical values for angles and position shifts based on photos and right: resulting position shifts based on the evaluation of the wetted areas.

Nozzle		$\alpha (x)$	$\alpha (y)$	x -shift (mm)	y -shift (mm)	x -shift (mm)	y -shift (mm)
column	row						
Theoretical values							
2	1	14.4°	4.2°	-28.2	+8.1	-25.4	+5.7
3	2	5.8°	14.1°	-11.1	-27.6	-12.6	-26.1

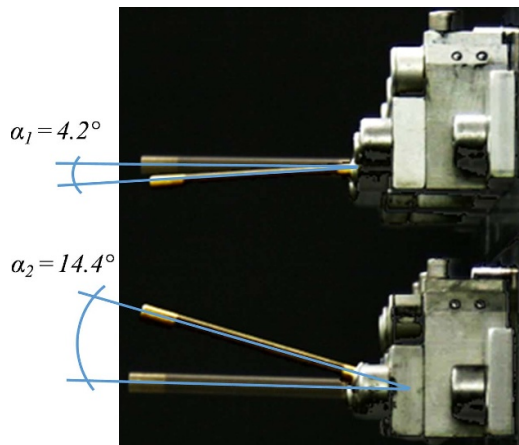


Figure 8. Side view of the top two lines of the nozzle-array to indicate the change in nozzle orientation. For this purpose, pins were locked to the nozzles with the changed orientation. The before and after images are superimposed.

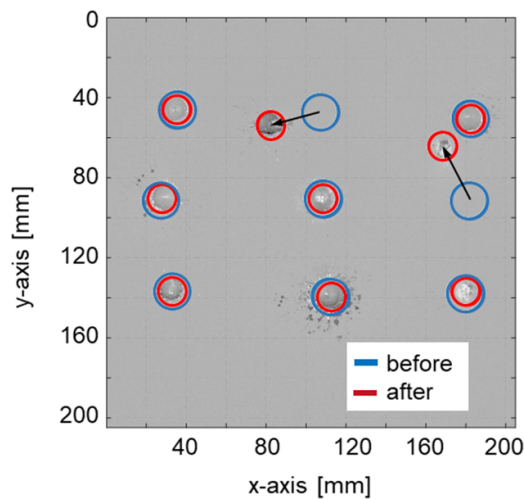


Figure 9. Comparison of center positions of wetted areas before and after a modification in the alignment of the nozzles for straight water injection.

An image of the wetted area resulting from the nozzle adjustment is shown in figure 9. In the picture, the positions of the centers are marked by circles, blue circles for the original positions and red circles for the new positions. The resulting changes in the position of the two adjusted nozzles can be easily traced. Based on such a picture alone, a technician could draw conclusions about the correct alignment of the nozzles.

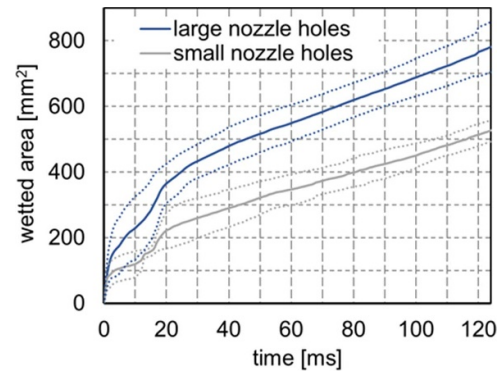


Figure 10. Progression of the wetted area as mean values of six nozzles with large holes and three nozzles with small holes on ten repetitions with straight water injection, while standard deviation is marked with dotted lines.

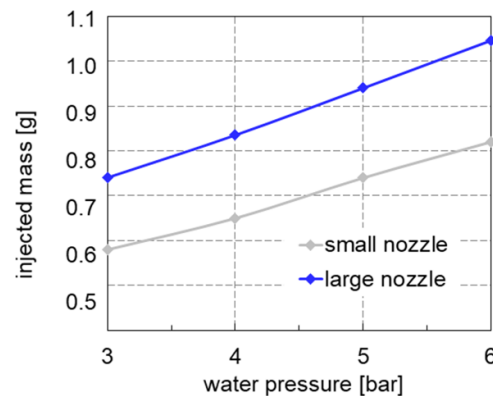


Figure 11. Injected mass over water pressure for an injection duration of 150 ms.

Before and after the adjustment the centers of the wetted areas were determined with the help of the evaluation algorithm. The difference in x - and y -direction are again shown in table 4 on the right-hand side.

The first nozzle (second column and first row) changes its orientation by 25.4 mm to the left and 5.7 mm downwards. In contrast, the second nozzle (third column and second row) changes its orientation by 12.6 mm to the left and 26.1 mm upwards. The nozzles which have not been changed show changes of a maximum of 0.7 mm to the original position. Thus, the changes in the alignment of the two nozzles are detectable.

It is now interesting to compare this with the theoretically determined values. For the first nozzle (second column

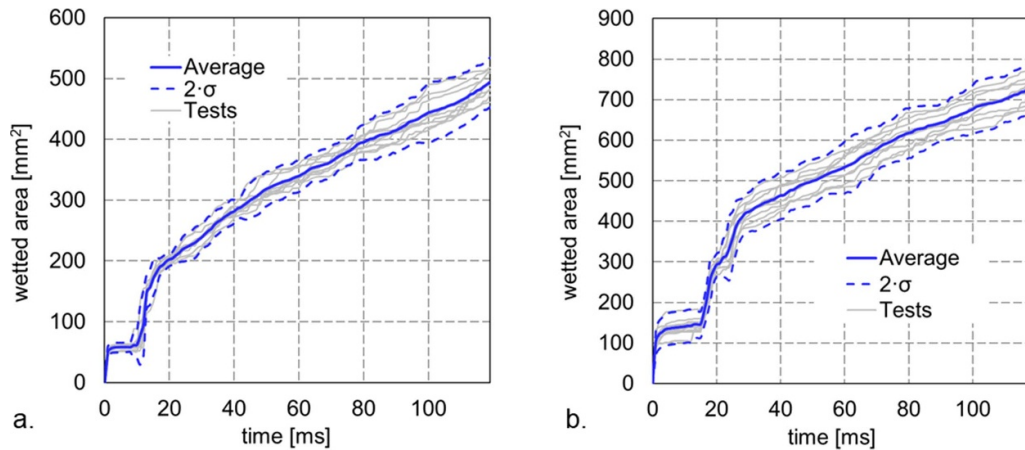


Figure 12. Progression of the wetted areas with ten repetitions including the average value and the twofold standard deviation; (a) small nozzle (column 2, row 3); (b) large nozzle (column 1, row 3).

and first row), it can be seen that the theoretically determined values differ from the values determined by the algorithm for the center point by 2.8 mm in the x -direction and by 2.4 mm in the y -direction. For the second nozzle (third column and second row), the difference in the x - and y -direction is only 1.5 mm. The differences can have various causes. For example, the optical determination of the angles by the pictures is accompanied by an uncertainty. Since only one photo was taken at a time and thus only one determination was made, random errors are not determined. In summary, it can be said that changes in alignment are easily detectable. However, it is difficult to draw precise conclusions about the adjustment angles, since determining the true adjustment angle is subject to errors.

3.3. Determination of the size of the wetted areas

In practical application, it would be of great advantage to be able to see whether the flow rate of a single nozzle changes during the operation of a spraying tool in a harsh foundry environment. To draw conclusions about the change in flow rate, the size of the wetted area can be used as a parameter. The determination of the wetted areas of the individual nozzles is carried out under the same conditions as the determination of the centers. Figure 10 shows the mean area progression over time for straight water injection. The mean value of the six large nozzles and the four small nozzles is plotted, including the corresponding standard deviations.

As binarized images are used for the evaluation, it must be taken into account that very small areas are initially removed by erosion. Thus, the areas are only recognized as wetted areas when a certain size is exceeded. This leads to a steep increase in the areas at the beginning. The following variations up to 30 ms can be explained by the different behavior of individual nozzles. For example, some induce a larger area faster than others do, due to the individual opening processes of the nozzles.

It can be seen that large nozzles produce a larger wetted surface. This is because the larger nozzles provide a larger mass flow rate, which allows the higher masses to take up a larger wetted area. In the diagram, the group of large nozzles has a bigger standard deviation (dotted lines), compared to the group of small nozzles. In the later course of the process after about 30 ms, an almost linear increase in the area occurs with both nozzle types.

In addition to the area measurements, we also measured the amount of water injected. Therefore, the injected water was collected in a reserve and balanced on a high precision balance. To collect a reasonable amount of water at each measurement point ten injections were performed. As an additional parameter the water pressure was varied between 3 and 6 bar. Considering an injection duration of 150 ms. Figure 11 shows that with increasing water pressure the injected mass increases as well. It is also clear that less water escapes from the small nozzles than from the large ones. If the injected quantity is related to a time period of 150 ms, the mass flow at 4 bar is 4.3 g s^{-1} for the small nozzles and 5.6 g s^{-1} for the large ones.

Since we know that the large nozzles produce a larger mass flow, it can be accepted that the differences in the size of the wetted area are due to differences in mass flow. Following the line of thought, for example, a partial clogging of the nozzle hole would lead to a reduction of the mass flow and a further reduction of the wetting surface can be expected. Besides, we have carried out preliminary studies in which we have systematically investigated the influence of water pressure. As expected, increased water pressure leads to larger wetting areas.

To derive information on individual nozzles figure 12 shows examples of the variance of the progression of the wetted areas. From a statistical point of view, the twofold standard deviation for a large number of tests will include 95% of all measured values. In the linear range for times greater than 30 ms, the twofold standard deviation adopts values between 6% and 10% relative to the average value. From this, it can be concluded that for a single test injection it is only possible to detect a disturbance within a nozzle if the wetted area during

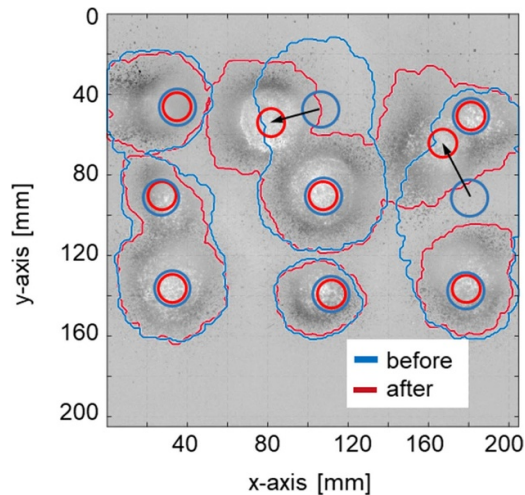


Figure 13. Comparison of spray impingement for the controlled test case with the realignment of two nozzles for the injection of a spray including boundaries found by pattern recognition algorithm; for the possibility of comparison, the previously determined positions of the centers of the straight water injection are also entered with circles.

the test measurement deviates more than 10% from a previously determined average value. If smaller deviations are to be detected, multiple injections must be made to determine an average value.

Based on the results, it is shown that with straight water injection, the size of the wetted surface of a nozzle can be measured and determined for each time step. If during a regular single shot control measurement of a spraying tool it turns out that the size of a wetted area changes by more than 10%, this will most likely be due to changes in the water-bearing system or the nozzle hole itself. The belonging nozzle can then be specifically maintained or replaced.

Finally, figure 13 displays the difficulties of the area determination injecting a spray using a complete nozzle array. The image is taken from the controlled test case with the realignment of two nozzles. Already after a short time, the wetted areas of the individual nozzles run into each other and form larger connected regions. These regions can be found by applying a pattern recognition algorithm.

With this result, it is not possible to draw conclusions about each nozzle automatically, but qualitative information is given to the user. Based on such an image a technician could draw conclusions about the correct function of the air-bearing system of the spraying tool, but further progress in post-processing is necessary, to automatically evaluate such an image.

4. Conclusions

In many industrial applications, there is a need for a measuring technique to control and document the correct function of multi-nozzle spraying tools. This measuring technique should be inexpensive, fast, reproducible and robust against harsh industrial conditions. It is not essential to determine quantitative measurement values such as droplet sizes, speeds or mass

flows. Rather, it is only necessary to determine whether the spraying tool behaves in the same way as at the time of commissioning (i.e. beginning of the tool life cycle when the spray tool was fully functional). We have developed such a measuring technique and examined its properties in more detail. For this purpose, a characteristic wetting pattern is generated by injecting on a frosted pane. If there are changes in the wetting pattern between the master image and the control image, this can be attributed to changes in the spraying tool. The test object in this study was a spraying tool with nine external mixing air-water nozzles, the geometric alignment of which is freely adjustable.

It was found that the functioning of the water-bearing system and the geometric alignment of the nozzles can be determined very precisely using the straight water injection. In the present setup, the maximum standard deviation of the center positions of the evaluated wetted areas was determined to be 0.35 mm. Therefore, a change in position or problems in the water-carrying system can already be inferred if the determined change in the center position of a single test injection is less than 1 mm.

With the help of a test case, in which the alignment of two nozzles was changed in a defined way, this could be confirmed. At the same time, changes in mass flow are detectable via a change in the size of the wetted areas.

The function of the air-guiding system which serves to atomize the water jet was tested by injecting full spray jets with the atomizing air switched on. On the one hand, changes in the center points of the wetted areas can be used to detect a partial disturbance of the air-bearing system of the individual spraying nozzles. On the other hand, the measurement results allow us to draw conclusions from the qualitative pattern of the wetted area. However, this analysis still requires a technician to interpret the wetting pattern. Future investigations will concentrate on developing the post-processing with the objective of extracting even more information from the images and further automating the image evaluation.

ORCID iDs

Florian Schulz  <https://orcid.org/0000-0002-7818-2823>

Frank Beyrau  <https://orcid.org/0000-0002-8043-7194>

References

- Ainsalo A, Sallinen R, Kaario O and Larimi M 2019 Optical investigation of spray characteristics for light fuel oil, kerosene, hexane, methanol and propane *Atomiz Sprays* **29** 521–44
- Aísa L, García J A, Cerecedo L M, García Palacín I and Calvo E 2002 Particle concentration and local mass flux measurements in two-phase flows with PDA. Application to a study on the dispersion of spherical particles in a turbulent air jet *Int. J. Multiph. Flow* **28** 301–24
- Baetz W, Holzapfel W, Dietrich H and Nath B 2005 Beam configuration for light sheet application *Measurement* **38** 42–52
- Beygi S, Kafashan M, Bahrami H R and Mugler D H 2012 The iterative shrinkage method for impulsive noise reduction from images *Meas. Sci. Technol.* **23** 114009

- Dannigkeit F, Steinke L and Ripperger S 2012 Inline-messung des mittleren tropfendurchmessers und der tropfenkonzentration von Prozesssprays *Chem. Ing. Tech.* **84** 357–64
- Dullenkopf K, Willmann M, Wittig S, Schöne F, Stieglmeier M, Tropea C and Mundo C 1998 Comparative mass flux measurements in sprays using a patternator and the phase-doppler technique *Part. Part. Syst. Charact.* **15** 81–89
- Elkottb M M, Rafat N M and Hanna M A 1978 The influence of swirl atomizer geometry on the atomization performance *Proc. 1st Int. Conf. Liq. At. Spray Syst.* 1978 pp 109–15
- Fansler T D and Parrish S E 2015 Spray measurement technology: a review *Meas. Sci. Technol.* **26** 12002
- Heldmann M, Knorsch T and Wensing M 2013 Investigation of fuel atomization and evaporation of a DISI injector spray under homogeneous charge conditions *SAE Int. J. Eng.* **6** 1213–21
- Henkel S, Beyrau F, Hardalupas Y and Taylor A M K P 2016 Novel method for the measurement of liquid film thickness during fuel spray impingement on surfaces *Opt. Express* **24** 2542–61
- ImochaSingh O, Sinam T, James O and Romen Singh T 2012 Local contrast and mean thresholding in image binarization *IJCA* **51** 4–10
- Khudeev R 2005 A new flood-fill algorithm for closed contour *2005 Siberian Conf. on Control and Communications. 2005 Siberian Conf. on Control and Communications (Tomsk, Russia, 21–22 October 2005)* (IEEE) pp 170–4
- Kim D, Park S S and Bae C 2018 Schlieren, Shadowgraph, Mie-scattering visualization of diesel and gasoline sprays in high pressure/high temperature chamber under GDCI engine low load condition *Int. J. Automot. Technol.* **19** 1–8
- Kumar J and Shunmugam M S 2006 Morphological operations on engineering surfaces using a 3D-structuring element of an appropriate size *Meas. Sci. Technol.* **17** 2655–64
- Lazzaro M and Ianniello R 2018 Image processing of vaporizing GDI sprays: a new curvature-based approach *Meas. Sci. Technol.* **29** 15402
- Lefebvre A H and McDonell V G 2017 *Atomization and Sprays* 2nd edn (Boca Raton, FL: CRC Press)
- Liu C, Liu F, Yang J, Yong M, Chunyan H and Gang X 2019a Experimental investigations of spray generated by a pressure swirl atomizer *J. Energy Inst.* **92** 210–21
- Liu H, Wang J, Duan H, Cai C, Jia M and Zhang Y 2019b Experimental study on the boiling criterion of the fuel film formed from spray/wall impingement *Exp. Fluids* **60** 13076
- Liu L, Jia Z, Yang J and Kasabov N K 2019c SAR image change detection based on mathematical morphology and the K-means clustering algorithm *IEEE Access* **7** 43970–8
- Lujaji F C, Boateng A A, Schaffer M, Mtui P L and Mkilaha I S N 2016 Spray atomization of bio-oil/ethanol blends with externally mixed nozzles *Exp. Therm. Fluid Sci.* **71** 146–53
- Mafi M, Martin H, Cabrerizo M, Andrian J, Barreto A and Adjouadi M 2019 A comprehensive survey on impulse and Gaussian denoising filters for digital images *Signal Process.* **157** 236–60
- May K R 1950 The measurement of airborne droplets by the magnesium oxide method *J. Sci. Instrum.* **27** 128–30
- Miller P C H and Butler Ellis M C 2000 Effects of formulation on spray nozzle performance for applications from ground-based boom sprayers *Crop Prot.* **19** 609–15
- Nazlibilek S, Karacor D, Ercan T, Sazli M H, Kalender O and Ege Y 2014 Automatic segmentation, counting, size determination and classification of white blood cells *Measurement* **55** 58–65
- Pan B, Qian K, Xie H and Asundi A 2009 Two-dimensional digital image correlation for in-plane displacement and strain measurement: a review *Meas. Sci. Technol.* **20** 62001
- Paredes-Orta C A, Mendiola-Santibañez J D, Manriquez-Guerrero F and Terol-Villalobos I R 2019 Method for grain size determination in carbon steels based on the ultimate opening *Measurement* **133** 193–207
- Rahim E A and Dorairaju H 2018 Evaluation of mist flow characteristic and performance in minimum quantity lubrication (MQL) machining *Measurement* **123** 213–25
- Serra J 1982 Image analysis and mathematical morphology [1] Image analysis and mathematical morphology vol 1 (London: Academic)
- Serras-Pereira J, Aleiferis P G and Richardson D 2015 An experimental database on the effects of single- and split injection strategies on spray formation and spark discharge in an optical direct-injection spark-ignition engine fuelled with gasoline, iso-octane and alcohols *Int. J. Eng. Res.* **16** 851–96
- Shedd T A and Newell T A 1998 Automated optical liquid film thickness measurement method *Rev. Sci. Instrum.* **69** 4205–13
- Steinmüller J 2008 Von der Bildverarbeitung zur räumlichen Interpretation von Bildern *Bildanalyse (eXamen.press)* (Berlin: Springer) (<https://doi.org/10.1007/978-3-540-79743-2>)
- von Deschwanden I, Benra F-K, Dohmen H J and Brillert D 2017 PDA measurements in spray generated by twin-jet-nozzles *Fluids Engineering Division Summer Meeting (Waikoloa, Hawaii, USA, July 30–August 3, 2017)* vol 1B (<https://doi.org/10.1115/FEDSM2017-69003>)
- Yokoi N and Aizu Y 2009 Methods for measuring refractive index and absorption coefficient of a moving particle using polarized-type phase-Doppler technique *Measurement* **42** 1352–62
- Zelenak M, Foldyna J, Scucka J, Hloch S and Riha Z 2015 Visualisation and measurement of high-speed pulsating and continuous water jets *Measurement* **72** 1–8
- Zhang M, Min X, Zhang Y, Zhang G and Cleary D J 2012 Flow-field investigation of multi-hole superheated sprays using high-speed PIV. Part I. Cross-sectional direction *Atomiz. Sprays* **22** 983–95